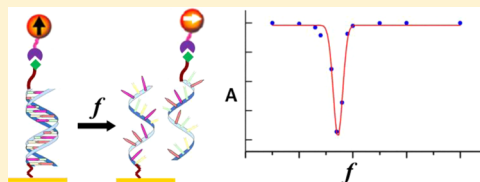


Well-Defined and Sequence-Specific Noncovalent Binding Forces of DNA

Lashan De Silva,[†] Li Yao,[†] Yuhong Wang,[‡] and Shoujun Xu^{*†}[†]Department of Chemistry and [‡]Department of Biology and Biochemistry, University of Houston, Houston, Texas 77204, United States

S Supporting Information

ABSTRACT: The specific binding between the two DNA strands in a double helix is one of the most fundamental and influential molecular interactions in biochemistry. Using force-induced remnant magnetization spectroscopy (FIRMS), we obtained well-defined binding forces of DNA oligomers, with a narrow force distribution of 1.8 pN. The narrow force distribution allows for directly resolving two DNA duplexes with a single base-pair difference in the same sample. Therefore, binding force can serve as a discriminating parameter for probing different DNA interactions. Furthermore, we observed that the binding forces depend on the position of the mismatching base pair. Our results show that FIRMS is capable of high-precision mechanical measurements of biochemical processes involving multiple DNA interactions and has the potential for characterizing the binding strength of materials based on DNA origami.



INTRODUCTION

Noncovalent binding between the two DNA or RNA strands in a double helix is one of the most important molecular interactions in chemistry and the life sciences.^{1–4} Furthermore, the sequence-specific binding between DNA strands has been used for molecular sensing^{5,6} and the construction of novel composite materials.^{7,8} Therefore, investigating the binding forces of DNA/RNA is of both fundamental significance and practical merit. Extensive research has been devoted to investigating DNA/RNA binding forces, primarily using atomic force microscopy (AFM)^{9–11} and optical tweezers.^{12–14} These techniques have provided detailed information on the conformational changes and binding forces during DNA/RNA stretching and dissociation. The force resolution of optical tweezers has reached sub-piconewton (pN).¹² However, the resulting force distribution is generally broad, on the order of 10 pN.^{14,15} In addition, some important cellular processes may be difficult to measure by these methods. For example, to measure the ribosome translocation, we have to apply an artificial hairpin RNA and substantial external force.¹⁶ Therefore, an open question is whether it is possible for a technique to measure a well-defined force with minimum invasion.

Recently, we reported a force-induced remnant magnetization spectroscopy (FIRMS) technique that uses an external mechanical force to distinguish specific antibody–antigen noncovalent bonds from nonspecific physisorption.¹⁷ The technique is based on the following concept: the magnetically labeled ligand molecules undergo Brownian motion once they dissociate from the receptor molecules, randomizing the magnetic orientations of the particles and consequently decreasing the magnetization. The binding force between an antibody–antigen pair has been measured, which was substantially higher than the binding force of physisorption.¹⁸

However, it remains unknown whether our technique can resolve different noncovalent bonds. One ultimate test for revealing force resolution will be measuring the binding forces of DNA duplexes because their binding forces can be finely tuned by changing the sequences and because extensive experimental work and theoretical modeling are both available for comparison.

Here we show the feasibility of determining well-defined, sequence-specific binding forces for DNA duplexes by using the FIRMS technique. The binding forces have a very narrow distribution. Multiple DNA interactions with only one base-pair (bp) difference can be completely resolved. In addition, DNA strands that differ only in the position of a mismatched base may have different binding forces. The results will have significant impact on fundamental biochemical research, theoretical modeling, and other applications.

EXPERIMENTAL METHODS

The atomic magnetometer has been described elsewhere.¹⁹ In brief, it uses the interaction between polarized Cs atoms and a linear-polarized laser beam. The Cs atoms in vapor phase in a glass cell ($5 \times 5 \times 5 \text{ mm}^3$) are first polarized by the laser. Then, the polarized atoms undergo Larmor precession in the magnetic field to be measured and consequently rotate the polarization of the laser light. The modulation frequency ω of the polarization rotation is equal to $2\gamma B$, where γ is the gyromagnetic ratio of Cs (3.5 Hz/nT) and B is the magnetic field. Therefore, the magnetic field can be determined by the frequency response of the optical rotation signal.

Received: April 17, 2013

Revised: May 23, 2013

Published: June 4, 2013

A sample well ($4 \times 2 \times 1 \text{ mm}^3$) with a gold-coated bottom surface was loaded with $8 \mu\text{L}$ of $10 \mu\text{M}$ single-stranded thiolated oligonucleotides $5'$ -thiol-GGG TTT TTT GGG- $3'$ (IDT DNA) in 10 mM tris(hydroxymethyl)aminomethane, 1 mM EDTA (TE-solution) and 1 M NaCl solution of pH 8.0 for 2 h. After rinsing with water, the sample well was immersed in $8 \mu\text{L}$ of 1 mM mercaptohexanol for 1 h, rinsed in deionized water, and dried again under nitrogen. For hybridizing, the cell was incubated with a solution of biotinylated probing strand, with sequences $5'$ -CCC AAA AAA CCC- $3'$ (complementary), CCC GAA AAA CCC (ninth-mismatched), $5'$ -CCC AGA AAA CCC- $3'$ (eighth-mismatched), or $5'$ -CCC AAG AAA CCC- $3'$ (seventh-mismatched). The sample well was then immersed in a 1% (w/v) bovine serum albumin (BSA) solution in tris-buffered saline (TBS) solution containing 0.05% of the detergent Tween 20 for 2 h. After incubation with $8 \mu\text{L}$ of streptavidin-coated magnetic particles (Invitrogen, M280) for 3 h, the sample well was immersed in a heat block at $65 \text{ }^\circ\text{C}$ for 5 min and cooled overnight. The sample was magnetized for 2 min using a permanent magnet after the incubation. The magnetizations of the magnetic particles were measured by an atomic magnetometer.

Figure 1a shows a schematic of the experimental setup. One of the strands, termed the target strand, is immobilized on a

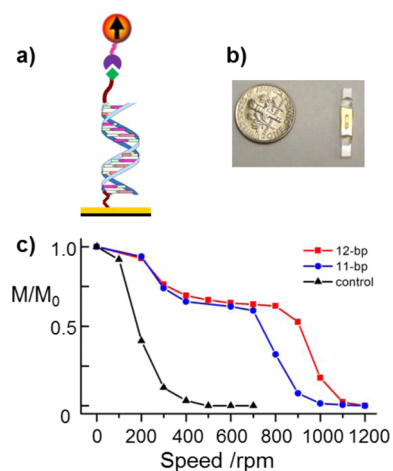


Figure 1. Dissociation of DNA duplexes using the FIRMS technique. (a) Schematic of the setup. (b) Photo of the sample well. (c) Plots of relative magnetization versus shaking force for two different DNA duplexes, one 12 bp and one 11 bp, plus a mismatched pair and a control. M_0 is the initial magnetization.

gold-coated surface via gold–sulfur bonds.²⁰ The other strand, the probing strand, is labeled with a magnetic particle via biotin–streptavidin coupling. A surface area of $4 \times 2 \text{ mm}^2$ of the sample well contains tens of thousands of such magnetically labeled DNA duplexes. Mechanical forces with increasing amplitudes, provided by a shaker (VWR, 12620-942) or a centrifuge (Eppendorf 5417R), are then applied to induce the dissociation of the double strands. After each force, the magnetization M of the magnetic particles is measured by an atomic magnetometer using a scanning magnetic imaging scheme (Supporting Information, Figure S1).²¹ Figure 1b shows a photo of the sample well with a U.S. dime to illustrate the scale.

RESULTS AND DISCUSSION

Figure 1c shows the results of testing a single type of DNA binding in the sample, using a shaking force to induce dissociation. For the 12-bp binding, the target strand was $5'$ -GGG TTT TTT GGG- $3'$, and the probing strand was $5'$ -CCC AAA AAA CCC- $3'$, which was fully complementary to the target strand. For the 11-bp DNA binding, the target strand was the same as that for the 12-bp binding, but the probing strand was $5'$ -CCC GAA AAA CCC- $3'$, with one mismatched base at the ninth position (ninth mismatching). The magnetization profiles revealed that the dissociation force was 950 rpm (revolution per minute) for the 12-bp binding and 800 rpm for the 11-bp binding. The initial decreases at 200–300 rpm in both cases were due to nonspecific physisorption, confirmed by a control experiment in which the magnetic particles did not contain the probing strands.

For force calibration, we used centrifugal force to dissociate the ninth mismatching duplex. Figure 2a shows the relative

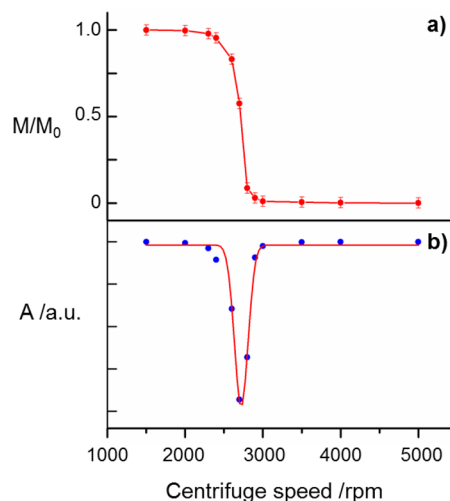


Figure 2. Force calibration and resolution for the 11-bp DNA binding. (a) Relative magnetization M/M_0 under various external forces measured as centrifuge speed. (b) Corresponding FIRMS spectrum and its Gaussian fitting. A : amplitude.

magnetization versus the centrifuge speed. The value of M at 1500 rpm is $1.29 \pm 0.04 \times 10^{-10} \text{ Am}^2$, which we define as M_0 to represent the total number of specifically bound magnetic particles (Supporting Information, Figure S1). The uncertainty indicates that the error for M/M_0 is typically 0.03 throughout this work. A sharp transition was observed between 2600 and 2800 rpm.

To obtain the precise force value for the dissociation, we took the derivative of the magnetization curve to obtain a FIRMS spectrum (Figure 2b). Fitting the spectrum with a single Gaussian function yielded a peak position of 2720 rpm. Therefore, the centrifugal force can be determined from $f = m\omega^2 r$, where m is the buoyant mass of the magnetic particles, ω is the angular velocity, and r is the distance of the particles from the rotation center.²² The M280 magnetic particles used here have a very narrow size distribution, which was verified by scanning electron microscopy (Supporting Information, Figure S2). From the particle diameter $2.54 \pm 0.07 \mu\text{m}$ and the density $1.52 \pm 0.02 \text{ g/mL}$, we determined the buoyant mass in the buffer solution (density 1.0 g/mL) to be $4.6 \times 10^{-15} \text{ kg}$. The peak position at 2720 rpm yields a ω value of 285 s^{-1} . For the

centrifuge used in this work, $r = 8.0$ cm. Therefore, the binding force for the 11-bp DNA duplex is 30 pN. The binding force for the 12-bp duplex can then be calculated using this value and the dissociation transitions in Figure 1c: $30 \times (950/800)^2 = 42$ pN. An independent force calibration for the 12-bp duplex was also performed using centrifugal force, which yields a binding force of 43 pN (Supporting Information, Figure S3).

The sharp transition in Figure 2 represents a very narrow distribution of the binding force, which indicates the high resolving capability for different noncovalent bonds with different binding forces. The resolving capability can be quantified from the half width at half-maximum of the Gaussian fit. The half width of the peak is 80 rpm, corresponding to $30 \times (2 \times 80/2720) = 1.8$ pN. The factor of 2 is because of the square dependence of force with respect to ω . For comparison, the typical half width of the force distribution by AFM is >5 pN.¹⁵

To verify that the dissociation of noncovalent bonds only occurs at a certain force, we performed kinetics measurements at two different centrifugal forces: one at 23 pN (2400 rpm) and one at 42 pN (3200 rpm), that is, before and after the above observed transition force of 30 pN, respectively. The results are shown in Figure 3. At 23 pN, the magnetization

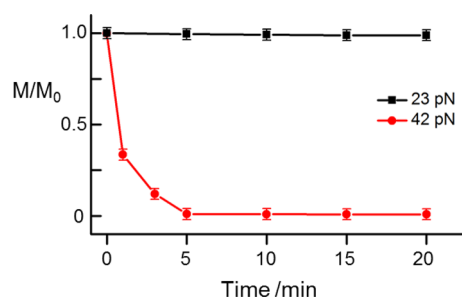


Figure 3. Dissociation time at two different force amplitudes, 23 and 42 pN, for the 11-bp DNA duplex.

remained high and unchanged for as long as 20 min; no bond dissociation took place. At 42 pN, the magnetization was reduced to zero within 5 min, and the magnetization remained zero thereafter. This result confirms that the dissociation of the DNA duplex occurs only when the external force exceeds the well-defined binding force. We also attempted 10 min duration for each force value and obtained results similar to Figure 2 (Supporting Information, Figure S4). The peak position of 2716 rpm was consistent with the 2720 rpm value in Figure 2. This also confirms the result in Figure 3 that the binding force is well-defined.

We attempt to compare the binding force values with those obtained from AFM and optical tweezers. The 12-pN difference between the 11-bp and 12-bp duplexes agrees well with both the results by AFM and optical tweezers: the AFM results showed that the force required to dissociate an A–T pairing is 9 ± 3 pN,²³ which is the difference between the two sequences here; optical tweezers showed 10–15 pN force during the unzipping of DNA.²⁴ In addition, our result of 42 pN for the 12-bp duplex agrees well with the literature value of 40 pN for a similar duplex of 5'-CGC TTT TTT GCG-3' binding its complementary sequence, obtained by AFM at a high loading rate of force.²⁵ Interestingly, theoretical work showed that at high loading rates the bond strength reached a plateau.²⁶ AFM operating in the force-clamp mode has similar experimental

condition to our FIRMS technique, in which a constant force is applied instead of a constant loading rate.²⁷ However, it has been mainly used for studying protein folding, not DNA rupture.^{28,29} Thermodynamic analysis indicates that a minimum of approximately eight base pairs is required to have a stable DNA duplex. Our force values, 30 pN for 11-bp and 42 pN for 12-bp, are in line with this analysis and a detailed AFM study.³⁰

A significant feature of our force spectra is that they are much narrower than the results obtained by AFM. This difference may be due to two possible reasons. One is that FIRMS simultaneously measures a large number of bonds. On the basis of the magnetization value of $1.29 \pm 0.04 \times 10^{-10}$ Am² and the magnetization calibration curve of the magnetic particles, we calculated that $9.5 \pm 0.6 \times 10^4$ bonds underwent dissociation (Supporting Information, Figure S5). This number is approximately two orders of magnitude higher than the typical number of events measured by single-molecule techniques such as AFM. Another possible reason could be the labeling with microparticles. Similar to our narrow force-induced dissociation, sharp melting profiles have been observed, in which DNAs were labeled with gold nanoparticles.³¹ Further investigation is needed to clarify this effect by using magnetic particles with different sizes and size distributions.

The well-defined binding force with an ultranarrow distribution makes it possible to distinguish different DNA interactions for very similar sequences. To demonstrate the unprecedented resolving capability, we made a 1:1 mixture of the two probing strands used in Figure 1c to form both the 12-bp and 11-bp DNA duplexes with the common target strand. Two distinct decreases were obtained (Figure 4). The plateau

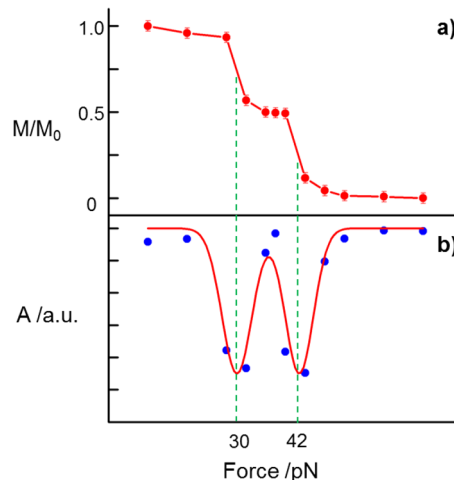


Figure 4. Resolving the binding forces of two different DNA duplexes with only one base-pair difference. (a) Relative magnetization versus calibrated external mechanical force. (b) Corresponding FIRMS spectrum.

between the two transitions is located at 50% M/M_0 , consistent with the ratio of the two probing strands (Figure 4a). The corresponding FIRMS spectrum in Figure 4b shows fully resolved two peaks. Compared with a previous AFM study with single bp resolution,³⁰ our work is able to directly reveal different DNA interactions without using a sophisticated model for data analysis. Different DNA interactions are also quantitatively obtained. The ability to resolve different DNA interactions in a single sample will allow FIRMS to be

employed in biochemical research that involves multiple DNA interactions.

High-resolution force spectroscopy also provides accurate force measurements to aid in the theoretical modeling of DNA interactions. We studied two more probing strands, with sequences 5'-CCC AGA AAA CCC-3' and 5'-CCC AAG AAA CCC-3', respectively, in addition to the ninth-mismatched strand. These two strands differ from the ninth-mismatched strand only in the position of the mismatched base G. We called the two strands the eighth-mismatched and the seventh-mismatched strands, respectively. The force measurements in Figure 5 show that the binding forces of the eighth-mismatched

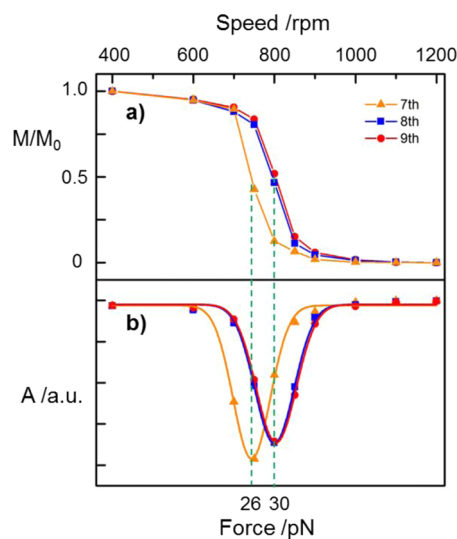


Figure 5. Binding forces of three DNA duplexes that differ only at the position of one base. (a) Relative magnetization versus calibrated external mechanical force. (b) Corresponding FIRMS spectrum.

and ninth-mismatched 11-bp duplexes are the same, while the binding force of the seventh-mismatched duplex is slightly lower. From the transitions at 800 rpm for the eighth-mismatched and ninth-mismatched duplexes and at 750 rpm for the seventh-mismatched duplex, we deduced the binding force of the latter to be $30 \times (750/800)^2 = 26$ pN, which is 4 pN lower than the binding forces of the other two strands.

To verify the small binding force difference between the seventh-mismatched duplex and the eighth-/ninth-mismatched duplexes, we used centrifugal force to directly obtain the binding force of the seventh-mismatched duplex (Supporting Information, Figure S6). From the fitted peak position of 2510 rpm, the binding force is calculated to be 26 pN, consistent with the force value previously obtained. This result confirms the small thermodynamic difference of the seventh-mismatched duplex compared with the eighth-/ninth-mismatched duplexes.

To quantitatively correlate our measured binding forces with thermodynamic parameters, we calculated the ΔG for the duplexes involved in this work. They were -13.29 and -10.97 kcal/mol for the 12-bp and ninth-mismatched 11-bp, respectively.³² The 12 pN difference in binding forces and 2.32 kcal/mol difference in ΔG between the two duplexes match well with thermodynamic prediction in which 13 pN force corresponds to ~ 2.2 kcal/mol energy.³³ However, although the ΔG values are identically -10.24 kcal/mol for both the eighth-mismatched and seventh-mismatched 11-bp duplexes based on the nearest-neighbor model,³² their binding

forces differ by 4 pN. This might be attributed to the slightly different π stacking in the two duplexes, which involves more than just the nearest base pairs.^{34,35} For example, in the eighth mismatched duplex there are four consecutive T–A pairs, which do not exist in the seventh-mismatched duplex. Xia et al. reviewed duplexes with identical nearest-neighbor base pairs but different thermodynamic stabilities and proposed an expanded nearest-neighbor model to predict thermodynamic parameters more precisely.³⁶ Our results of precise force measurements support the necessity of a more accurate model.

The FIRMS technique uses different magnetic properties of the tagged magnetic particles to identify bound and dissociated states. This unique technical feature allows us to noninvasively probe and resolve different molecular interactions, which is an advantage over AFM. However, AFM is able to provide dynamic conformational changes of the bound molecules during stretching, whereas FIRMS detects only the initial bound state and the final dissociated state. We also compare FIRMS to other techniques, for example, optical microscopy. One advantage for magnetic-based FIRMS is that the sample system does not need to be perfectly transparent, which is required for optical-based techniques. In addition, the magnetic property difference clearly indicates the molecular binding states. Rebinding of the dissociated magnetic particles is unlikely because the dissociated particles are physically removed from the reaction area by the mechanical force. In addition, the Brownian relaxation time of the magnetic particles is shorter than 1 s.³⁷

CONCLUSIONS

In conclusion, we report well-defined, sequence-specific binding forces for DNA duplexes using the recently invented FIRMS technique. The force distribution is as narrow as 1.8 pN. This feature enables resolving multiple DNA bindings that differ only in one base within the same sample. The high force resolution also reveals that DNA binding forces depend on the position of the mismatched base. This work shows that FIRMS is capable of resolving different DNA–DNA interactions and protein–DNA/RNA bindings in biological processes in future studies as well as characterizing the binding strength of DNA-based exotic materials.

ASSOCIATED CONTENT

Supporting Information

Magnetization measurement, characterization of the magnetic particles, additional force measurements, and quantification of the dissociated bonds. This material is available free of charge via the Internet at <http://pubs.acs.org>.

AUTHOR INFORMATION

Corresponding Author

*Email: sxu7@uh.edu (S. X.).

Notes

The authors declare no competing financial interest.

ACKNOWLEDGMENTS

The authors acknowledge support from National Science Foundation under grant ECCS-1028328 and from Texas Center for Superconductivity at the University of Houston (S.X.). This work is partially supported by the Welch Foundation under grant E-1721 (Y.W.), a GEAR grant (S.X.), and the McElrath Fellowship (L.Y.).

■ ABBREVIATIONS

DNA, deoxyribonucleic acid; FIRMS, force-induced remnant magnetization spectroscopy; AFM, atomic force microscopy

■ REFERENCES

- (1) Chaurasiya, K. R.; Paramanathan, T.; McCauley, M. J.; Williams, M. C. Biophysical Characterization of DNA Binding from Single Molecule Force Measurements. *Phys. Life Rev.* **2010**, *7*, 299–341.
- (2) Bustamante, C.; Bryant, Z.; Smith, S. B. Ten Years Of Tension: Single-Molecule DNA Mechanics. *Nature* **2003**, *421*, 423–427.
- (3) Brenner, M. D.; Zhou, R.; Ha, T. Force a Connection: Impacts of Single-Molecule Force Spectroscopy on In Vivo Tension Sensing. *Biopolymers* **2011**, *95*, 332–344.
- (4) Sharp, P. A. RNAi and Double-Strand RNA. *Genes Dev.* **1999**, *13*, 139–141.
- (5) Severin, P. M. D.; Ho, D.; Gaub, H. E. A High Throughput Molecular Force Assay for Protein-DNA Interactions. *Lab Chip* **2011**, *11*, 856–862.
- (6) Wang, H.; Yang, R.; Yang, L.; Tan, W. Nucleic Acid Conjugated Nanomaterials for Enhanced Molecular Recognition. *ACS Nano* **2009**, *3*, 2451–2460.
- (7) Macfarlane, R. J.; Lee, B.; Jones, M. R.; Harris, N.; Schatz, G. C.; Mirkin, C. A. Nanoparticle Superlattice Engineering with DNA. *Science* **2011**, *334*, 204–208.
- (8) Rajendran, A.; Endo, M.; Sugiyama, H. Single-Molecule Analysis Using DNA Origami. *Angew. Chem., Int. Ed.* **2012**, *51*, 874–890.
- (9) Lee, G. U.; Chrisey, L. A.; Colton, R. J. Direct Measurement of the Force Between Complementary Strands of DNA. *Science* **1994**, *266*, 771–773.
- (10) Krautbauer, R.; Rief, M.; Gaub, H. E. Unzipping DNA Oligomers. *Nano Lett.* **2003**, *3*, 493–496.
- (11) Strunz, T.; Oroszlan, K.; Schäfer, R.; Güntherodt, H.-J. Dynamic Force Spectroscopy of Single DNA Molecules. *Proc. Natl. Acad. Sci.* **1999**, *96*, 11277–11282.
- (12) Bockelmann, U.; Thomen, Ph.; Essevez-Roulet, B.; Viasnoff, V.; F. Heslot, F. Unzipping DNA with Optical Tweezers: High Sequence Sensitivity and Force Flips. *Biophys. J.* **2002**, *82*, 1537–1553.
- (13) Koch, S. J.; Shundrovsky, A.; Jantzen, B. C.; Wang, M. D. Probing Protein-DNA Interactions by Unzipping a Single DNA Double Helix. *Biophys. J.* **2002**, *83*, 1098–1105.
- (14) Ritchie, D. B.; Foster, D. A. N.; Woodside, M. T. Programmed –1 Frameshifting Efficiency Correlated with RNA Pseudoknot Conformational Plasticity, Not Resistant to Mechanical Unfolding. *Proc. Natl. Acad. Sci. U.S.A.* **2012**, *109*, 16167–16172.
- (15) Ho, D.; Zimmermann, J. L.; Dehmelt, F. A.; Steinbach, U.; Erdmann, M.; Severin, P.; Falter, K.; Gaub, H. E. Force-Driven Separation of Short Double-Stranded DNA. *Biophys. J.* **2009**, *97*, 3158–3167.
- (16) Qu, X.; Lancaster, L.; Noller, H. F.; Bustamante, C.; Tinoco, I. Ribosomal Protein S1 Unwinds Double-Stranded RNA in Multiple Steps. *Proc. Natl. Acad. Sci. U.S.A.* **2012**, *109*, 14458–14463.
- (17) Yao, L.; Xu, S.-J. Force-Induced Remnant Magnetization Spectroscopy for Specific Magnetic Imaging of Molecules. *Angew. Chem., Int. Ed.* **2011**, *50*, 4407–4409.
- (18) Yao, L.; Xu, S.-J. Force-Induced Selective Dissociation of Noncovalent Antibody-Antigen Bonds. *J. Phys. Chem. B* **2012**, *116*, 9944–9948.
- (19) Garcia, N. C.; Yu, D.; Yao, L.; Xu, S.-J. Optical Atomic Magnetometer at Body Temperature for Magnetic Particles Imaging and Nuclear Magnetic Resonance. *Opt. Lett.* **2010**, *35*, 661–663.
- (20) Wirtz, R.; Wälti, C.; Germishuizen, W. A.; Pepper, M.; Middelberg, A. P. J.; Davies, A. G. High-Sensitivity Colorimetric Detection of DNA Hybridization on a Gold Surface with High Spatial Resolution. *Nanotechnology* **2003**, *14*, 7–10.
- (21) Yao, L.; Xu, S.-J. Long-Range, High-Resolution Magnetic Imaging of Nanoparticles. *Angew. Chem., Int. Ed.* **2009**, *48*, 5679–5682.
- (22) Halvorsen, K.; Wong, W. P. Massively Parallel Single-Molecule Manipulation Using Centrifugal Froce. *Biophys. J.* **2010**, *98*, L53–L55.
- (23) Rief, M.; Clausen-Schaumann, H.; Gaub, H. E. Sequence-Dependent Mechanics of Single DNA Molecules. *Nat. Struct. Biol.* **1999**, *6*, 346–349.
- (24) Bockelmann, U.; Thomen, P.; Heslot, F. Dynamics of the DNA Duplex Formation Studied by Single Molecule Force Measurements. *Biophys. J.* **2004**, *87*, 3388–3396.
- (25) Pope, L. H.; Davies, M. C.; Laughton, C. A.; Roberts, C. J.; Tendler, S. J. B.; Williams, P. M. Force-Induced Melting of a Short DNA Double Helix. *Eur. Biophys. J.* **2001**, *30*, 53–62.
- (26) Evans, E.; Ritchie, K. Dynamic Strength of Molecular Adhesion Bonds. *Biophys. J.* **1997**, *72*, 1541–1555.
- (27) Fernandez, J. M.; Li, H. B. Force-Clamp Spectroscopy Monitors the Folding Trajectory of a Single Protein. *Science* **2004**, *303*, 1674–1678.
- (28) Garcia-Manyes, S.; Brujic, J.; Badilla, C. L.; Fernández, J. M. Force-Clamp Spectroscopy of Single-Protein Monomers Reveals Individual Unfolding Pathways of I27 and Ubiquitin. *Biophys. J.* **2007**, *93*, 2436–2446.
- (29) Capitanio, M.; Canepari, M.; Maffei, M.; Beneventi, D.; Monaco, C.; Vanzi, F.; Bottinelli, R.; Pavone, F. S. Ultrafast Force-Clamp Spectroscopy of Single Molecules Reveals Load Dependence of Myosin Working Stroke. *Nat. Methods* **2012**, *9*, 1013–1019.
- (30) Sattin, B. D.; Pelling, A. E.; Goh, M. C. DNA Base Pair Resolution by Single Molecule Force Spectroscopy. *Nucleic Acids Res.* **2004**, *32*, 4876–4883.
- (31) Taton, T. A.; Mirkin, C. A.; Letsinger, R. L. Scanometric DNA Array Detection with Nanoparticle Probes. *Science* **2000**, *289*, 1757–1760.
- (32) SantaLucia, J.; Hicks, D. The Thermodynamics of DNA Structural Motifs. *Annu. Rev. Biophys. Biomol. Struct.* **2004**, *33*, 415–440.
- (33) Lavery, R.; Lebrun, A.; Allemand, J.-F.; Bensimon, D.; Croquette, V. Structure and Mechanics of Single Biomolecules: Experiment and Simulation. *J. Phys.: Condens. Matter* **2002**, *14*, R383–R414.
- (34) Šponer, J.; Jurečka, P.; Marchan, I.; Luque, F. J.; Orozco, M.; Hobza, P. Nature of Base Stacking: Reference Quantum-Chemical Stacking Energies in Ten Unique B-DNA Base-Pair Steps. *Chem.—Eur. J.* **2006**, *12*, 2854–2865.
- (35) Vanegas, P. L.; Horwitz, T. S.; Znosko, B. M. Effects of Non-Nearest Neighbors on the Thermodynamic Stability of RNA GNRA Hairpin Tetraloops. *Biochemistry* **2012**, *51*, 2192–2198.
- (36) Xia, T. B.; SantaLucia, J.; Burkard, M. E.; Kierzek, R.; Schroeder, S. J.; Jiao, X. Q.; Cox, C.; Turner, D. H. Thermodynamic Parameters for an Expanded Nearest-Neighbor Model for Formation of RNA Duplexes with Watson-Crick Base Pairs. *Biochemistry* **1998**, *37*, 14719–14735.
- (37) Chemla, Y. R.; Grossman, H. L.; Poon, Y.; McDermott, R.; Stevens, R.; Alper, M. D.; Clarke, J. Ultrasensitive Magnetic Biosensor for Homogeneous Immunoassay. *Proc. Natl. Acad. Sci. U.S.A.* **2000**, *97*, 14268–14272.